Journal of Photochemistry and Photobiology A: Chemistry 223 (2011) 25–36

Contents lists available at ScienceDirect

Journal of Photochemistry and Photobiology A: Chemistry

journal homepage: www.elsevier.com/locate/jphotochem

Self-association of a naphthalene-capped-β-cyclodextrin through cooperative strong hydrophobic interactions

M. José González-Álvarez[a], Alejandro Méndez-Ardoy[b], Juan M. Benito[c], José M. García Fernández[c], Francisco Mendicuti[a,*]

[a] Dpto. Química Física, Universidad de Alcalá, Edificio de Farmacia, Campus Universitario Ctra. Madrid-Barcelona Km 33,600, E-28871 Alcalá de Henares, Madrid, Spain
[b] Dpto. Química Orgánica, Universidad de Sevilla, Fac. de Química, E-41012 Sevilla, Spain
[c] Instituto de Investigaciones Químicas, CSIC–Universidad de Sevilla, E-41092 Sevilla, Spain

ARTICLE INFO

Article history:
Received 29 April 2011
Received in revised form 15 July 2011
Accepted 19 July 2011
Available online 26 July 2011

Keywords:
Cyclodextrins
Fluorescence
Circular dichroism
Molecular modelling
Hydrophobic effect

ABSTRACT

NMR, circular dichroism and fluorescence techniques were used to study the structure in solution of a new β-cyclodextrin derivate in which naphthalene chromophore group is bridged to O(2) and O(3) secondary positions of the same glucopyranose unit through a bidentate hinge. The results point to the formation of a very stable dimer in aqueous solution which dissociates in non-polar solvents. Dimerization was enthalpy and entropy favoured. The hydrophobic character of the naphthyl moiety plays a very important role in the entropy change sign. Molecular mechanics as well as molecular dynamics calculations indicated that the most stable dimers are head-to-head oriented. For these dimer structures the naphthyl moieties, relatively shielded from the solvent, are sufficiently close to each other to couple their transition moments, but without forming excimers.

1. Introduction

Cyclodextrins (CDs) are cyclic oligosaccharides composed of 6, 7 or 8 D-glucopyranose termed α, β and γCD, respectively. Because of their hydrophobic cavity, they are capable of forming inclusion complexes in water with a great variety of organic compounds [1,2], which makes them ideal for many supramolecular applications including drug delivery, sensors or molecular machines [2,3]. The utility of native CDs is often limited because of their relatively low discrimination character among guests of similar size, solubility, which is restricted to water or very polar solvents [4], and the conformational constrains imposed by the cyclooligosaccharide architecture. Efforts have been made to chemically modify natural CDs in order to manipulate their binding properties, enhance the enantioselectivity towards chiral guests, achieve solubility in a desired solvent or investigate the inclusion mechanism [5]. In this context, *O*-methylated CDs offer many advantageous features for applications in fields such as the separation of chiral molecules or drug encapsulation [6]. Thus, permethylated CDs exhibit a larger flexibility as compared to the native CDs, with a wider cavity and higher solubility in both aqueous and organic solvents [7–9].

Fluorescently labeled CD derivatives represent very useful tool for sensing applications and supramolecular studies. The attachment of a chromophore to a CD not only alters the original binding ability and selectivity, but also provides a spectroscopic probe for investigating the structure, conformations and the molecular recognition of multiple molecules [10–13]. The naphthalene group is particularly attractive for this purpose due to the numerous applications in photochemical molecular devices [14] and fluorescence molecular sensors [14–20]. Consequently, a great effort has been devoted to investigate the structure, conformation and aggregation properties in solution of naphthalene-modified CDs. Ueno et al. [21,22] have studied the self-inclusion processes of βCD bearing two naphthyl moieties linked to the primary CD face. One of the two pendant naphthyl moieties seems to move outwards–inwards from the inner cavity. Equilibrium is reached between a predominant form in which a naphthyl group is included into the CD cavity and another one where both naphthyl groups are located outside. The conformational changes in the appended group, which were monitored by excimer fluorescence and circular dichroism, were guest-dependent. Valeur's group [23–25] have reported the photophysical properties of βCDs bearing several 2-naphthoyloxy chromophores substituted at one or both CD faces. These systems were used as a model for studying the excitation energy transfer process among naphthalene moieties. Garcia-Garibay and McAlpine [16,26,27] described the synthesis and the inside-outside isomerism of 3-O-(2-methylnaphthyl)-βCD.

* Corresponding author. Tel.: +34 918854672; fax: +34 918854763.
E-mail address: francisco.mendicuti@uah.es (F. Mendicuti).

1010-6030/$ – see front matter © 2011 Elsevier B.V. All rights reserved.
doi:10.1016/j.jphotochem.2011.07.013

^{1}H NMR experiments revealed the presence of dimers at concentrations higher than 0.1 mM. The circular dichroism spectrum of diluted samples was, however, consistent with a monomer form. ^{1}H NMR chemical shift variations as a function of concentration provided a monomer–dimer equilibrium constant of 5000 M^{-1} at 25 °C [16]. Other authors [17,18] have studied how the differences in the chain length of the linker of the appended naphthyl group to the CD affect the association behaviour of the modified βCD. The presence of dimers for the 6-O-mono-2-naphthoate βCD, where the 2-naphthoyl moiety is directly attached to the CD, was demonstrated. However, when the chromophore group is connected to the CD through a relatively long chain as in 6-[(*N*-2-naphthoyl-2-aminoethyl)amino]-6-deoxy βCD the molecule prefers to adopt a self-inclusion conformation. Park et al. have also synthesized CD derivates bearing different chromophoric moieties [15,19,20], among which the 6-O-(2-sulfonate-6-naphtyl)-βCD. This compound exhibits a monomer–dimer equilibrium with a high dimerization constant (~10^4 M^{-1} at 25 °C) [28,29]. The naphthyl group did not present an excimer band in the fluorescence spectra but it did show an exciton coupling band in the circular dichroism spectrum which denotes a relative proximity between naphthyl moieties. More recently, Liu et al. [11] have reported the synthesis of two novel permethylated βCD derivates containing naphthalene and quinoline appended groups. The results from circular dichroism and ROESY spectra showed that both chromophores are deeply self-included into the cavity of the CD. Nevertheless, both groups are expelled towards the narrow primary face upon complexation of bile salt guests.

A common characteristic of the above commented works is that the chromophore substituent is linked to a single glucopyranose position at either the primary or the secondary rim. The conformational and aggregation properties in solution are then dictated by the ability to form intra- or intermolecular inclusion complexes. However, we have reported the self-association processes of 2^I,3^I-*O*-(*o*-xylylene)-permethylated CDs (X*m*CD) in which a xylylene chromophore group bridged simultaneously vicinal O(2) and O(3) of the same glucopyranose [30–32]. Small dimerization equilibrium constants were obtained (K_D: ~180, ~200 and 248 M^{-1} for X*m*α-, -β- and -γCDs, respectively, at 25 °C). Dimerization processes were accompanied by $\Delta H < 0$ and $\Delta S < 0$. Molecular dynamics simulations for X*m*CD monomers demonstrated the presence of an *open* (or *half-open*)/*capped* equilibrium which is significantly displaced to the *open* conformation. Calculations also revealed that the most stable dimers are those formed when two X*m*CDs approach through their secondary faces (head-to-head, *HH*).

In addition, the X*m*CDs shows negative solubility coefficients in water, being more soluble in cold than in hot water. This situation is analogous at that observed for per-*O*-methylated and partially methylated CD derivatives [33]. X-ray studies in this series suggest that the reverse solubility as compared with canonic CDs is due to the breakdown of hydration networks leading to aggregation [34–41]. Although this particular behaviour can be attributed, in essence, to the hydrophobic effect, the crystallographic studies alone do not allow determining the pathway which leads from high solubility in cold water to low solubility at higher temperature. The presence of the doubly linked aromatic ring in X*m*CDs seems to exacerbate this effect, favouring the formation of well-defined dimeric species in solution through a mechanism that does not involve inclusion phenomena. These modified CDs may thus serve as well-defined systems to study the hydrophobic effect in more deep by using spectroscopic techniques.

This work describes the synthesis and study the behaviour in water of a hinge-type capped CD named 2^I,3^I-*O*-(1,8-naphtylene)-per-*O*-Me-β-cyclodextrin (N*m*βCD), which contains a naphthyl cap-like moiety. Dimerization equilibrium constant, thermodynamic parameters upon association and information about the structure in water were obtained by using NMR, fluorescence, circular dichroism and molecular modelling techniques. The complexation of 1,8-dimethoxynaphatalene (*o*N) [42] and the hetero-association of N*m*βCD both with heptakis(2,3,6,-tri-*O*-methyl)βCD (MeβCD) were also studied.

To the best of our knowledge, this is the first report on a naphthyl appended CD derivative that self-aggregates by strong hydrophobic interactions with really large binding constants and without the need for inclusion of the substituent into the partner CD. Compared to βCD derivatives bearing a single-linked naphtyl substituent, the double-linked hinge-type disposition should impose significant conformational constraints. Notably, it forces a quasi-perpendicular disposition of the major axis on the naphthalene moiety and the central axis of the βCD molecule, disfavouring self-inclusion and/or penetration into the partner CD.

2. Experimental

2.1. Synthesis and characterization

Briefly, the synthesis of 2^I,3^I-*O*-(1,8-naphtylene)-per-*O*-Me-β-cyclodextrin (N*m*βCD), was accomplished in two steps starting from its xylylene-appended counterpart X*m*βCD [30] (Scheme 1). Catalytic hydrogenation of the benzylic ether furnished the selectively differentiated vicinal diol diOH*m*βCD which can be now reacted with an excess of 1,8-bis(bromomethyl)naphthalene in DMF in the presence of sodium hydride (Scheme 1). One-pot double alkylation furnished the target compound N*m*βCD (37% overall yield from X*m*βCD). The structures of the diOH*m*βCD intermediate and N*m*βCD were confirmed by NMR, electrospray mass spectra (ESIMS) and combustion analysis. Synthetic details as well as characterization data are included in Supporting Information (Figs. S4–S6).

2.2. Solution preparations, instruments and experimental details

The solutions of N*m*βCD used for fluorescence and circular dichroism experiments were prepared by weight in deionized water (Milli-Q) and stirred for ~24 h prior to measuring. The concentrations ranged from 0.002 to 0.4 mM. For the aqueous solution of MeβCD the concentration range was wider reaching concentrations close to 11 mM. All the organic solvents used in the fluorescence and circular dichroism experiments were spectroscopic or purity > 98% grades. Nevertheless they were always checked before use. 2,3-Butanedione (diacetyl, Aldrich) was used as fluorescence quencher for the naphthyl group. Sodium 1-adamantanecarboxylate (AC) and/or adamantyl-1-amine (AA) were also used as control guest molecules to probe the accessibility to the βCD cavity in water. 1,8-Bis(methoxymethyl)naphthalene (*o*N) was prepared as previously described from the corresponding 1,8-bis(hydroxymethyl) naphthalene [43].

^{1}H NMR, 2D COSY, 1D NOESY and 1D TOCSY experiments were performed by using a 500 MHz, Bruker 500 DRX instrument in the 5–60 °C temperature range. For NMR measurements solutions of N*m*βCD in deuterated water were prepared in the 1.42–22 mM range. Though the lowest concentration was still above the detection limit for this particular compound, no significant spectral changes were observed by working below 1 mM. For NMR titration experiments, 1.5 mM stock solutions of N*m*βCD in D_2O were prepared. A 500-μL aliquot of the stock solution was transferred to a 5-mm NMR tube, and the initial NMR spectrum was recorded. A solution (10–20 mM) of the guest (AC or AA) in the previous stock solution of N*m*βCD was then prepared. Aliquots of this solution were gradually added to the NMR tube via microsyringe, recording the corresponding spectrum after each addition. Additions were

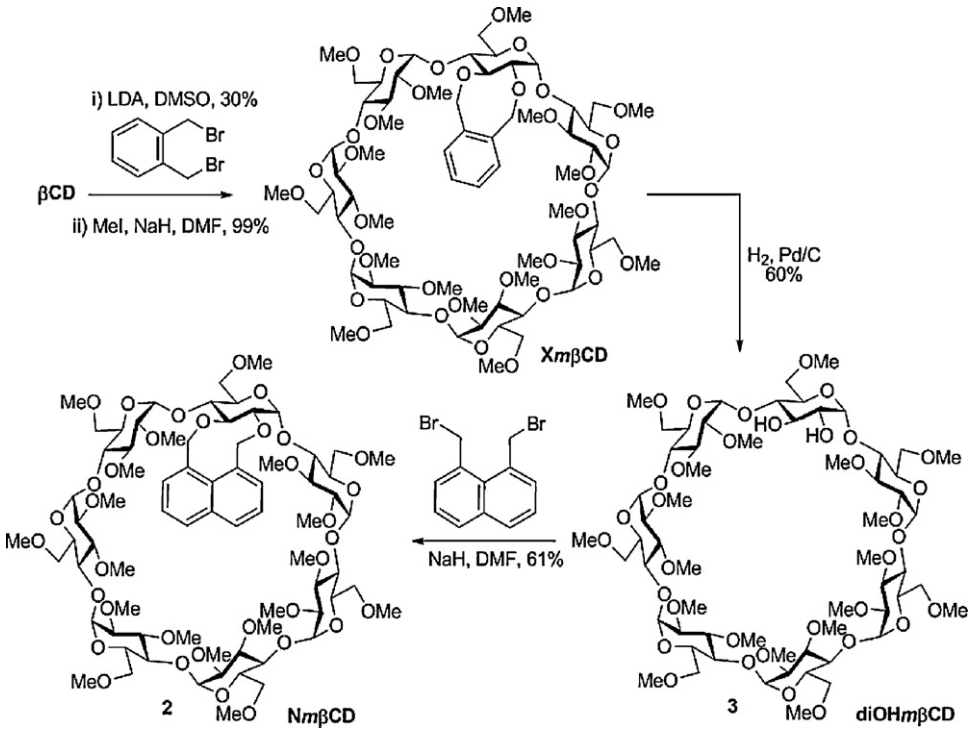

Scheme 1. Synthesis of, 2^{I},3^{I}-*O*-(1,8-naphthalene)-per-*O*-methyl-β-cyclodextrin (N*m*βCD) from 2^{I},3^{I}-*O*-(*o*-xylylene)-per-*O*-methyl-β-cyclodextrin (X*m*CDs).

continued until complete saturation of the host. Chemical shift variation of the host diagnostic signals were plotted against the guest concentration and binding constants were calculated from these data by using a least-squares fitting protocol [42].

Steady-state fluorescence was performed by using a high sensitivity spectrofluorimeter, the SLM 8100C Aminco, equipped with a cooled photomultiplier and a double (single) monochromator in the excitation (emission) path. The fluorescence decay measurements were achieved on a time correlated single photon counting (TCSPC) FL900 Edinburgh Instruments Spectrometer with a thyratron-gated lamp filled with H_2. Circular dichroism (ICD) spectra were obtained by using a JASCO-715 spectropolarimeter (see Supporting Information, *Instruments and Experimental Details*).

3. Results and discussion

3.1. Absorption spectra

As depicted in Fig. 1, the N*m*βCD absorption spectrum in water exhibits two intense main bands whose maxima are placed at 220 and 290 nm and a very faint one located at 320 nm. N*m*βCD/water solutions show spectra that very well match the one observed for the *o*N model compound but whose maxima are slightly shifted to the blue by about 4 nm. By comparison the of *o*N structure with similar naphthalene derivates [44,45], these bands can be ascribed, according to Platt's notation [46], to the $^{1}B_b$, $^{1}L_a$ and $^{1}L_b$ electronic transitions. For these transitions dipole moments (superimposed in Fig. 1) are nearly parallel to the long ($^{1}B_b$) and short (both $^{1}L_a$ and $^{1}L_b$) naphthalene main axis.

3.2. Fluorescence measurements

3.2.1. Emission spectra

Fig. 2 shows the emission spectra for N*m*βCD/water solutions upon excitation of the naphthyl group at 295 nm. Each spectrum exhibits a double band located at ~335 and ~342 nm and a shoulder at ~355 nm. The fluorescence intensity obviously increases upon increasing the N*m*βCD concentration, but this fact does not affect the ratio between the intensities of the two main bands. This, in addition to the fact that the spectra never showed a broadening to the red, denotes the absence of any intermolecular naphthalene excimers.

The association constant K_D for the dimerization process of N*m*βCD described by the equilibrium:

$$2\,\mathrm{N}m\beta\mathrm{CD} \rightleftarrows (\mathrm{N}m\beta\mathrm{CD})_2 \quad (1)$$

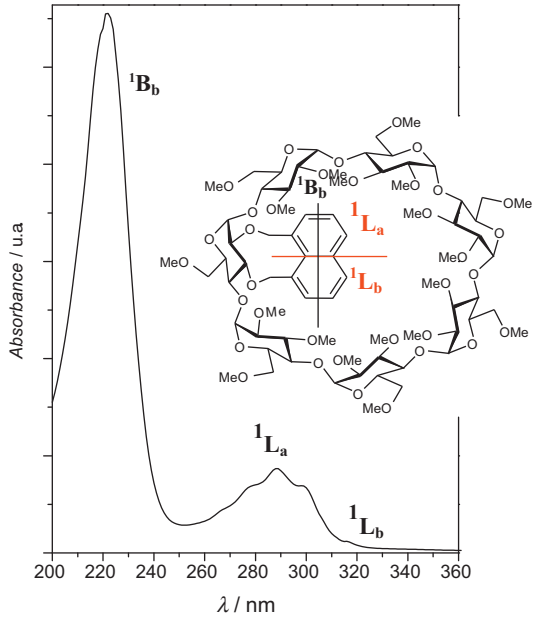

Fig. 1. Absorption spectra for N*m*βCD in water dilute solution at 25 °C. Superimposed is the N*m*βCD structure showing the directions of the electronic transitions moments.

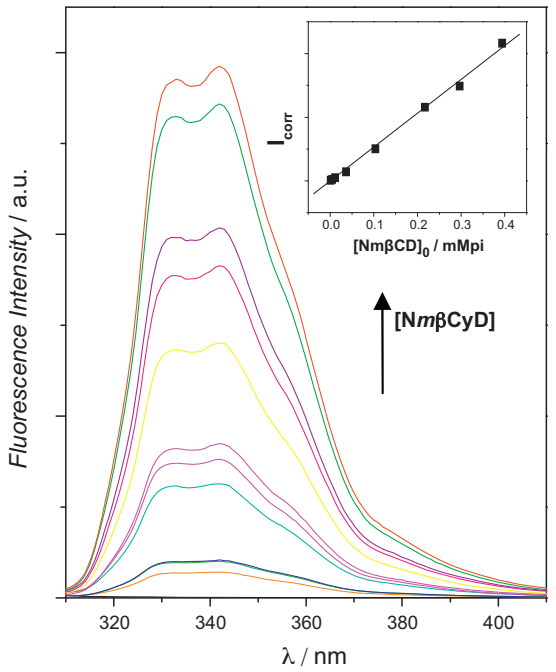

Fig. 2. Emission spectra (λ_{ex} = 295 nm) for N*m*βCD/water solutions in the 0–0.425 mM range of concentrations at 25 °C. Changes of the corrected fluorescence intensity with [N*m*βCD] at 25 °C are superimposed.

can be related with the fluorescence intensity (I) measured as the area under the naphthyl group emission spectrum, and the total N*m*βCD concentration by Eq. (2) [31]:

$$I = \phi_{(\mathrm{Nm\beta CD})_2}[\mathrm{Nm\beta CD}]_0 - \left(\phi_{(\mathrm{Nm\beta CD})_2} - \phi_{\mathrm{Nm\beta CD}}\right)\frac{\left(\sqrt{8K_D[\mathrm{Nm\beta CD}]_0 + 1} - 1\right)}{4K_D} \quad (2)$$

where $\phi_{(\mathrm{Nm\beta CD})}$ and $\phi_{(\mathrm{Nm\beta CD})_2}$ are the proportionality constants (per chromophore unit) between fluorescence intensity and concentration of the monomer and dimer forms.

A plot of the corrected fluorescence intensity taking into account the inner effect, (I_{corr}) with [N*m*βCD]$_0$ at 25 °C is inserted in Fig. 2 (more details in *Instruments and Experimental Details* in Supporting Information). This representation is linear and the $I_{corr}/[[\mathrm{Nm\beta CD}]_0$ ratio remains constant in the whole range of N*m*βCD concentrations used in our measurements. This fact demonstrates, according to Eq. (2), that $\phi_{(\mathrm{Nm\beta CD})_2} \cong \phi_{\mathrm{Nm\beta CD}}$, or in other words, the fluorescence quantum yield does not change with the dimerization process.

3.2.2. Fluorescence intensity decays

Time-resolved fluorescence measurements for N*m*βCD aqueous solutions at different concentrations and temperatures were performed at the maximum of the emission band (342 nm) upon excitation of the naphthyl group (295 nm).

The fluorescence intensity decay profiles were fitted to three-exponentials at any [N*m*βCD] and temperature [47]. The short lived component (~0.2 ns) was ascribed to the innate stray light and/or scattering of the cylindrical cuvettes used. The intermediate (~12 ns) and the slowest (~30 ns) components were assigned to the free (N*m*βCD) and the dimer (N*m*βCD)$_2$ species, respectively.

As shown in Fig. 3, the fractional contribution of the intermediate component decay time, $f_{\mathrm{Nm\beta CD}}$, (more details in *Instruments and Experimental Details* in Supporting Information), decreases with [N*m*βCD], whereas the contribution of the slowest component,

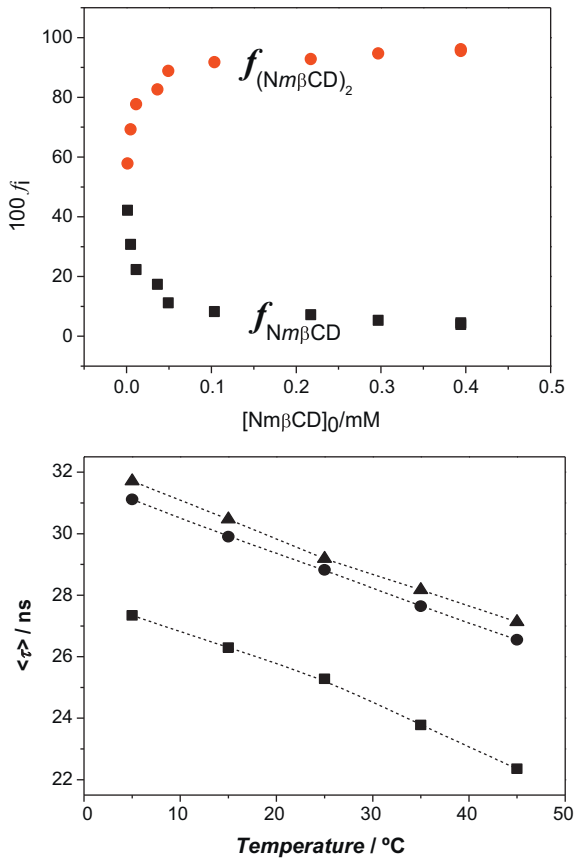

Fig. 3. (Upper) Changes with the concentration of the monomer (■) and dimer (●) fractions ($100 \times f_i$) obtained from the different lifetime contributions ascribed to both species. (Bottom) Variation of the weighted average lifetime with the temperature for [N*m*βCD] = 0.00479 (■), 0.104 (●) and 0.394 mM (▲). (For interpretation of the references to color in this figure legend, the reader is referred to the web version of the article.)

$f_{(\mathrm{Nm\beta CD})_2}$, increases and, in agreement with an enthalpy-favoured association process, it noticeably decreases with temperature due to complex dissociation. In consequence, the weighted average lifetimes $\langle\tau\rangle$ defined as:

$$\langle\tau\rangle = f_{\mathrm{Nm\beta CD}}\tau_{\mathrm{Nm\beta CD}} + f_{(\mathrm{Nm\beta CD})_2}\tau_{(\mathrm{Nm\beta CD})_2} \quad (3)$$

where $\tau_{\mathrm{Nm\beta CD}}$ and $\tau_{(\mathrm{Nm\beta CD})_2}$ are the lifetimes for both species, increase (decreases) with [N*m*βCD] (temperature) as inferred from Fig. 3.

3.2.3. Thermodynamics of the dimerization processes

The variation of the average lifetime ($\langle\tau\rangle$) against [N*m*βCD]$_0$ at different temperatures is depicted in Fig. 4. The $\langle\tau\rangle$ increasing with [N*m*βCD]$_0$ is due to the increase in the dimer fraction. The near plateau is achieved at very low concentrations pointing towards a high dimerization constant.

Additionally, these experimental data can be fit to the following non-linear equation [31]:

$$\langle\tau\rangle = \frac{2\tau_{\mathrm{Nm\beta CD}} + (\phi_{(\mathrm{Nm\beta CD})_2}/\phi_{\mathrm{Nm\beta CD}})\,\tau_{(\mathrm{Nm\beta CD})_2}\left(\sqrt{8K_D[\mathrm{Nm\beta CD}]_0 + 1} - 1\right)}{2 + (\phi_{(\mathrm{Nm\beta CD})_2}/\phi_{\mathrm{Nm\beta CD}})\left(\sqrt{8K_D[\mathrm{Nm\beta CD}]_0 + 1} - 1\right)} \quad (4)$$

The experimental data which fit reasonably to the curve generated by Eq. (4) under the assumption that $\phi_{(\mathrm{Nm\beta CD})_2}/\phi_{\mathrm{Nm\beta CD}} = 1$, provide association constants at different temperatures collected in Table 1. The K_D values obtained were significantly high in comparison with those calculated for similar naphthalene-substituted βCDs [16–18,28,29].

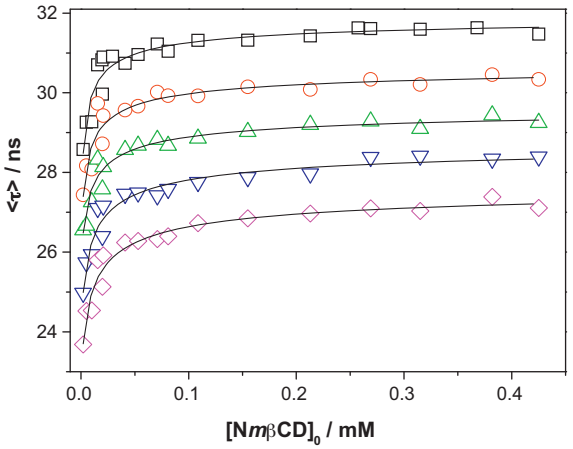

Fig. 4. Variation of the weighted average lifetime $\langle\tau\rangle$ with [N*m*βCD] water solutions at several temperatures: 5 °C (□); 15 °C (○); 25 °C (△); 35 °C (▽); 45 °C (◊).

Table 1
Association constants K_D, $\tau_{Nm\beta CD}$ and $\tau_{(Nm\beta CD)_2}$ parameters obtained from analysis of decay profiles at different [N*m*βCD] and temperatures.

T (°C)	10^{-3} K_D (M^{-1})	$\tau_{Nm\beta CD}$	$\tau_{(Nm\beta CD)_2}$
5	216 ± 202	26.5 ± 1.6	32.4 ± 0.2
15	137 ± 127	26.1 ± 1.2	30.8 ± 0.2
25	92 ± 58	25.5 ± 0.6	29.8 ± 0.2
35	78 ± 44	24.0 ± 0.6	28.9 ± 0.2
45	69 ± 34	22.8 ± 0.6	27.8 ± 0.2

The thermodynamic parameters for the dimerization process were attained from the van't Hoff linear representations (Fig. S1 in Supporting Information). Both ΔH (-21.3 ± 2.7 kJ mol^{-1}) and ΔS ($+24.7 \pm 9.2$ J K^{-1} mol^{-1}) parameters favour N*m*βCD dimerization. Intermolecular CD associations by attractive van der Waals or electrostatic interactions are usually characterized by $\Delta H < 0$. In fact, the value and sign of ΔH is very similar to that obtained for the dimerization process of X*m*βCD (and their X*m*αCD and X*m*γCD partners [31,32]) and also for the complexation of many other naphthalene derivates with βCDs [48–51]. The favourable positive value of ΔS for N*m*βCD, in contrast with the negative value found for X*m*βCD (and also for X*m*αCD and X*m*γCD [31,32]), must be due to the different size of the appended moiety and the higher hydrophobicity of a naphthyl group in aqueous medium, as compared to the benzyl group. For a dimerization process, the quantitative value and sign for ΔS is the result of the balance between two opposite factors: (i) the expected loss of degrees of freedom accompanying any self-assembling and (ii) the reorganization of host and guest solvating water molecules during the process [52]. The larger size of the naphthalene compared to the benzene, will cause a larger loss of solvating shells during N*m*βCD dimerization and consequently this effect will contribute more favourably to ΔS.

3.2.4. Fluorescence quenching

The fluorescence quenching experiments are quite useful to determine the accessibility of a free quencher to the naphthyl anchored to the βCD, giving information about its location. Quenching measurements by diacetyl were carried out on *o*N (very diluted) and N*m*βCD/water solutions at 25 °C. For the latter system two N*m*βCD concentrations (2.68×10^{-3} mM and 0.257 mM) were employed. At these concentrations and temperature the dimer molar fractions were approximately 0.15 and 0.8, respectively. Stern–Volmer $\langle\tau_0\rangle/\langle\tau\rangle$ plots were linear in the whole range of concentrations used. The Stern–Volmer constants (K_{SV}) were 40.9, 26.9 and 2.5 M^{-1} for *o*N and 2.68×10^{-3} mM and 0.257 mM N*m*βCD, respectively. The bimolecular quenching constants (k_q) [53] for each system were $(3.0 \pm 0.2) \times 10^9$, $(1.6 \pm 0.5) \times 10^9$ and $(8.5 \pm 0.6) \times 10^7$ M^{-1} s^{-1}, respectively. These results demonstrate that naphthyl moiety in the isolated *o*N is obviously much more accessible to the quencher than in the N*m*βCD dimer, where it is probably shielded by the two CD macrorings (or perhaps partially included into the partner CD). As expected, k_q values drastically decreases with the dimer fraction. In addition, the temperature dependence on k_q was obtained for the 0.257 mM N*m*βCD/water solution. k_q's of $(3.7 \pm 0.2) \times 10^7$, $(8.5 \pm 0.6) \times 10^7$ and $(1.9 \pm 0.2) \times 10^8$ M^{-1} s^{-1} for 5 °C, 25 °C and 45 °C, respectively, were in agreement with $\Delta H < 0$.

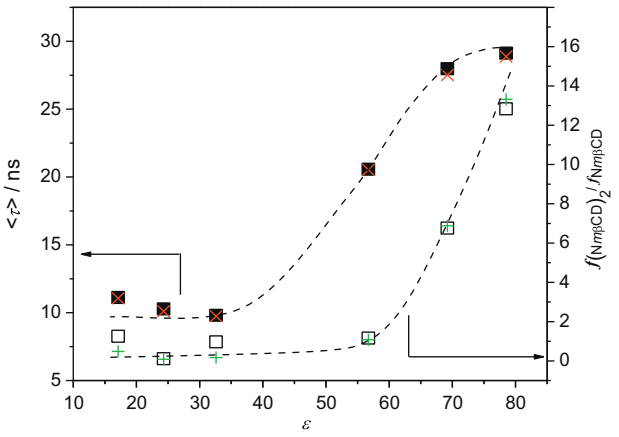

Fig. 5. Changes in the lifetime averages ($\langle\tau\rangle$) (■) and the fractional dimer-to-monomer contribution ratios (□) with ε for fluorescence decay measurements performed on N*m*βCD 0.2 mM solutions of different solvents: water, methanol/water (20:80 and 50:50, v/v), methanol, ethanol and butanol at 25 °C. Idem upon adding AC up to reaching a 1.6 M concentration (× and +, respectively).

3.2.5. Dependence of the fluorescence quantum yield and lifetime with medium polarity (ε) and microviscosity (η)

The influence of the medium ε and η on the fluorescence quantum yield (Φ) and lifetime (τ) for the naphthyl moiety in N*m*βCD was assessed by measuring dilute solutions of the *o*N model in several solvents (water, methanol/water, ethanol/water mixtures and *n*-alcohols) at 25 °C. The results (Fig. S2, Supporting Information) reveal that in the case of the *o*N derivative τ decreases with ε, for $\varepsilon > 50$, and it increases with η. Φ, however, does not show any special trend when varying ε and η ($\Phi \approx 0.08 \pm 0.06$). Dimer formation in N*m*βCD may involve a decreasing (increasing) in polarity (microviscosity) surrounding the chromophore (appended naphthyl placed between both CDs or perhaps included in the inner cavity of a βCD partner whose $\varepsilon \approx 50$ [32]). These results may therefore agree with $\tau_{(Nm\beta CD)_2} > \tau_{Nm\beta CD}$ and with $\phi_{(Nm\beta CD)_2} \cong \phi_{Nm\beta CD}$.

Fluorescence decay measurements on N*m*βCD solutions in different polarity solvents were also performed. The concentrations used were similar in all experiments, [N*m*βCD] ≈ 0.2 mM (dimer molar fraction ~0.8). Fig. 5 depicts the ratio of the fractional contributions for decay times attributed to the dimer and monomer species and $\langle\tau\rangle$ variations with ε. Results indicate a decrease in both the fractional ratio values and $\langle\tau\rangle$ when decreasing the solvent polarity as a consequence of the dissociation of the $(Nm\beta CD)_2$ into the monomer species with a faster lifetime component.

On the other hand, it is well known the large affinity of adamantane derivatives for βCD by forming 1:1 strong stable complexes ($K \sim 10^4$ M^{-1}) in water [12,54–56]. Processes like self-inclusion of CD appended groups, dimer formation or any other guest complexation may compete with this strong complexation. Sodium 1-adamantanecarboxylate (AC) was added to each of the previously studied N*m*βCD (0.2 mM) solutions up to reaching [AC] = 1.6 mM

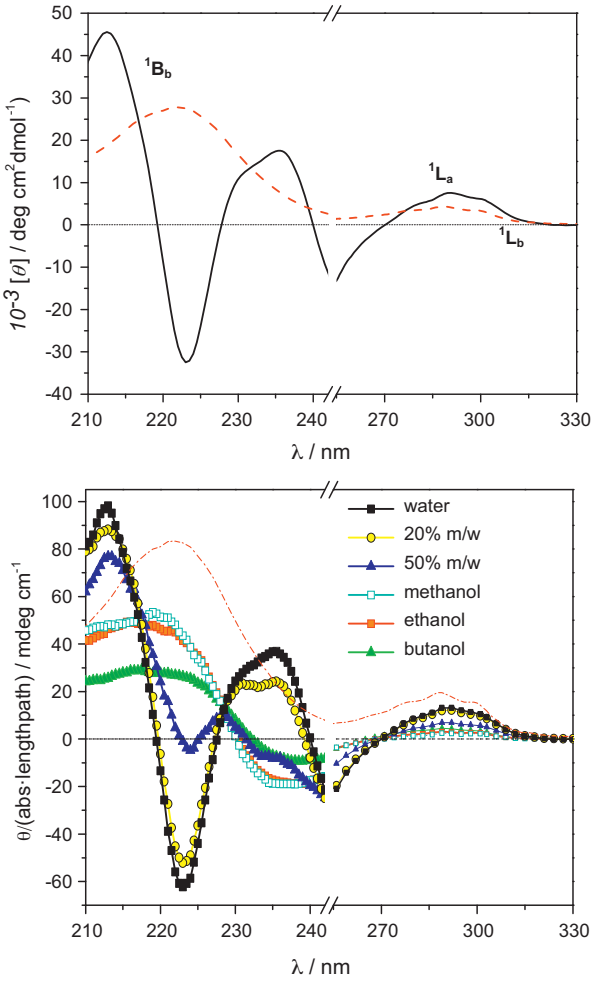

Fig. 6. Absorption spectra ( ) and circular dichroism ( ) for N*m*βCD (0.2 mM in water) at 25 °C (upper); comparative circular dichroism spectra for N*m*βCD solution of a different polarity solvent at 25 °C ([N*m*βCD] ≈ 0.2 mM) (bottom). (For interpretation of the references to color in this figure legend, the reader is referred to the web version of the article.)

(8-fold excess). Results are also represented in Fig. 5 and show that the addition of excess AC does not produce any significant changes neither in ⟨τ⟩, nor in the fractional dimer-to-monomer contribution ratios whatever the polarity of the solvent was.

3.3. Circular dichroism measurements

The magnitude and sign of the ICD spectrum of a chromophore guest when it interacts with a CD can inform about its location with respect to the CD [57–61]. The ICD spectrum sign varies depending on the type and depth of the guest inclusion in the CD cavity and the orientation of its electronic transition moment relative to the CD *n*-fold axis. Parallel (perpendicular) orientation gives a positive (negative) ICD band which becomes opposite sign when the chromophore is located partially outside [57–61].

Fig. 6 (upper) shows the circular dichroism spectrum of N*m*βCD (0.2 mM in water) at 25 °C. At this concentration and temperature around the 80% of the N*m*βCD is in dimer form. The ICD spectrum exhibits a relatively intense exciton coupling (EC) band in the electronic ^1B_b transition region, whereas a slightly positive band is observed in the ^1L_a zone. ICD spectrum for EC is characterized by the typical bisignate Cotton effect that takes place when two chromophores are close enough to couple their electric transition moments. In general, stronger absorption and smaller interchromophore distances leads to larger intensity for the positive and negative peaks in the EC signal [62]. In case of a pair of naphthalene moieties, EC takes place when they are spaced out by around 7 Å [62]. Thus, EC signal observed for the ^1B_b band in water most probably points towards the presence of *HH*-type (N*m*βCD)$_2$ dimers in this solvent. Furthermore, this structure would be presumably stabilized through mutual cooperative interactions between the naphthyl groups, or even between naphthyl groups and secondary methyl groups, as predicted before for (X*m*CD)$_2$ dimers [30–32].

Different polarity solvent-induced circular dichroism variations on N*m*βCD were also examined and depicted in the bottom panel of Fig. 6. Variations in the solvent polarity (the same solvents and concentrations as in the previous section) made drastic changes in the ICD spectra band shape and intensities. Whereas the ^1L_a intensity band monotonically decreases when decreasing medium polarity (ε), the intensity of the EC dual band decreases down to methanol, and then, becomes a single positive band in less polar solvents. This means that when the medium surrounding N*m*βCD becomes more and more hydrophobic, the interaction between naphthyl groups turns weaker, shifting the equilibrium towards the monomeric species. The relatively intense positive ^1B_b and weak ^1L_a bands in the non-polar solvents would agree with a monomer N*m*βCD species where the naphthyl group, interacting with its CD macroring, would be located outside the cavity and lying relatively parallel to it, according to Kodaka's rules [57,59]. Similar conclusions were reached from lifetime measurements described earlier in this paper, where a decrease in medium polarity means an increase in the monomer fraction. These would also agree with the explanation given for the $\Delta S > 0$ for N*m*βCD dimerization in water, where the hydrophobic effect is assumed to play an important role.

As with fluorescence measurements, neither the intensity nor the shape at the ^1B_b or ^1L_a ICD bands were influenced by the addition of AC to the N*m*βCD solutions used in our previous experiments at 25 °C. Complexation of AC with N*m*βCD in polar solvents cannot compete with its strong self-association at 25 °C. Same behaviour was observed at 45 °C in water. Furthermore, the results also reflect that AC does not form inclusion complexes with N*m*βCD in non-polar solvents. Similar conclusions were reached from time-resolved measurements at 25 °C (or 45 °C).

The variation of the ICD with the concentration for N*m*βCD/water solutions for the ^1L_a band at 25 °C was also studied. Unfortunately, due to the low absorptivity of this band, it was not possible to get reliable ICD signals at concentrations smaller than 0.25 mM. For N*m*βCD concentrations larger than 0.25 mM only a slight variation in the ICD signal with [N*m*βCD] is observed, since the plateau, as shown in Fig. 4, is almost reached. Even so, the experimental data can reasonably be adjusted to a non-linear equation similar to Eq. (3), by using the K_D value obtained previously by fluorescence lifetime measurements at the same temperature [63].

3.4. Study of the heterodimerization process

To evaluate the role of the naphthyl moiety in the intermolecular self-association of N*m*βCD, the heterodimerization between N*m*βCD and permethylated βCD (MeβCD) at different temperatures was also studied. The results show a fairly small decrease in ⟨τ⟩ with [MeβCD]. At the [N*m*βCD] used, ~80% of N*m*βCD forms a very stable dimer, and even the addition of a great excess of MeβCD (up to ×70 times) does not force (N*m*βCD)$_2$ to dissociate, *i.e.* does not substantially decrease ⟨τ⟩. These results reinforce the idea that the mutual and strong cooperation between naphthyl groups is mainly responsible for the high (N*m*βCD)$_2$ stability. The study of the *o*N model complexation with MeβCD was also tackled. ⟨τ⟩ for *o*N/MeβCD water solutions ([*o*N] kept constant) also hardly change upon MeβCD addition at any temperature. *o*N nearly does not inter-

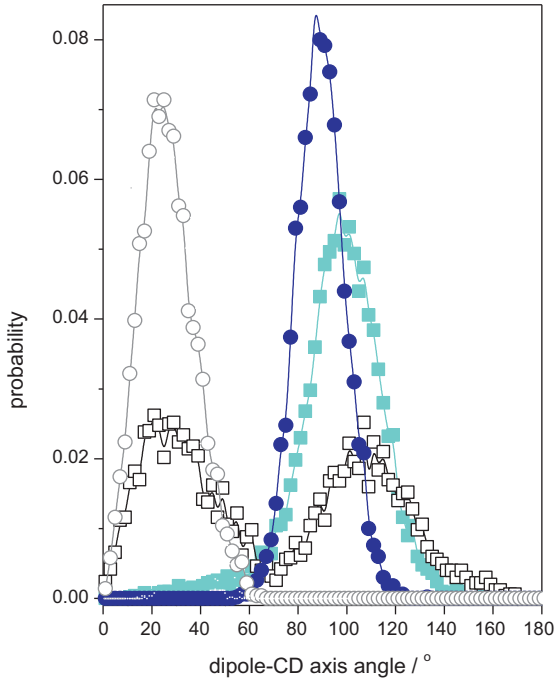

Fig. 7. Probability distributions of the angles between the 7-fold CD axis and ^1B_b (filled symbols) and ^1L_a (open symbols) electronic transition moments for naphthyl group obtained from the analysis of the 10 ns MD trajectories performed on N*m*βCD half-open (2) conformation at 350 K (circles) and 600 K (squares).

act with MeβCD or if it does, its binding constant is extremely low (Fig. S3 in the Supporting Information).

These experiments demonstrate that two interacting naphthyl groups are required to make a presumably *HH*-type dimer formation possible. It also supports that this interaction does not involve inclusion of the naphthalene moieties in the CD cavities. Circular dichroism also reinforces this fact. In both the N*m*βCD/MeβCD and *o*N/MeβCD experiments, the ICD spectra did not exhibit any variation with [MeβCD] either.

3.5. NMR measurements

In contrast to that reported for the analogous xylylene-tethered βCD counterpart [47–52], ^{1}H NMR spectra for N*m*βCD in D_2O at different concentrations (1.42–22 mM) and temperatures (5–50 °C) featured no significant proton chemical shift variations (see Fig. S7, Supporting Information). This observation fits with the remarkably high dimerization constant (K_D) determined by time-resolved fluorescence. In fact, the N*m*βCD concentrations used in NMR experiments exceed the concentrations at which, according to Fig. 4, any chemical shift variations must be observed. The scenario is similar to that encountered when ICD signal variation with [N*m*βCD] for the ^1L_a band was monitored.

The remarkable ^{1}H NMR spectrum signal splitting observed for N*m*βCD in D_2O solutions at 25 °C is ascribable to the large anisotropic effect induced by the naphthyl group and further supports that the naphthalene moiety is relatively close to the secondary rim of the CD torus in the dimer, so that all glucose protons become affected by the associated electronic current. Full assignment of the seven magnetically non-equivalent glucopyranosyl units was then possible by combining 2D COSY and 1D TOCSY experiments (Fig. S8, Supporting Information). The observation of cross-peaks in the NOE spectra between aromatic protons and methoxy groups at the secondary rim of the CD moiety (Fig. S9, Supporting Information) is also in agreement with the *HH* orientation of the two CD partners upon dimer formation.

Extensive precipitation occurred in D_2O solutions of N*m*βCD above 50–60 °C (depending on the concentration) resulting in line broadening in the NMR spectra, which probably indicates that the monomeric species, whose fraction increases with temperature ($\Delta H < 0$), is too insoluble in D_2O to allow detection by NMR.

The shape of the ^{1}H NMR spectrum for N*m*βCD collected in deuterated chloroform (1.5 mM at 25 °C) was sharply different to that registered in D_2O, with extensive overlapping of the signals, indicating that the naphthalene ring is probably more distant from the CD cavity and exposed to the solvent. The spectrum did not change with concentration or temperature, and no precipitation was observed. This agrees with the conclusions inferred from the fluorescence and ICD experiments indicating that monomeric species are mainly present in non-polar solvents.

The capability of N*m*βCD to form inclusion complexes in water with either adamantane-1-carboxilate (AC) or adamantyl-1-amine (AA) was also assayed by NMR. Virtually no changes on the proton chemical shifts of N*m*βCD were observed upon titration with either of the guests up to 10-fold molar excess, which denotes that complexation of AC or AA with N*m*βCD does not take place. This is sharply different to that previously observed for X*m*βCD or the permethylated βCD (MeβCD), which formed 1:1 complexes with AC (binding constants of $443 \pm 2\ M^{-1}$ and $965 \pm 15\ M^{-1}$, respectively, at 25 °C) [30]. This observation further supports the existence of an aggregate stabilized through hydrophobic interactions at relatively low temperatures, in which the access to the cavity is blocked.

3.6. Molecular mechanics and molecular dynamics calculations

Molecular mechanics (MM) and molecular dynamics (MD) calculations were performed with Sybyl 8.0 [64] and the Tripos Force Field [65]. A relative permittivity $\varepsilon = 3.5$ ($\varepsilon = 1$) was used in the vacuum (in the presence of water). Charges for N*m*βCD were obtained by MOPAC [66]. The starting N*m*βCD were built with the macroring in the non-distorted form ($\phi = 0°$ and $\psi = -3°$, $\tau = 121.7°$ and side chain χ angles in the *trans* conformation [67]) and the naphthyl substituent in some of the most probable conformations (ten) for the chain that links the naphthalene moiety to a glucopyranose unit of the βCD macroring. These ten selected conformations for N*m*βCD appended group were those of the minima potential energies (MBE) from a total of 400 starting conformations obtained by placement of the four torsional angles that describe the rotation around C(3)–O–CH_2–C^{ar}(1) and C(2)–O–CH_2–C^{ar}(8) ether bonds at the maxima of their probability distribution functions and further structures minimization. These distributions (depicted in Fig. S10, Supporting Information) were obtained from the analysis of the 10 ns MD trajectories (at 600 K) performed on an isolated glucopyranose linear trimer, where the central unit contains the bidentate naphthalene moiety substituted at the C(2) and C(3) positions (a description of the method is included in Supporting Information, page 21). Structure optimizations were carried out by the simplex algorithm, and the conjugate gradient was used as a termination method with gradients of 0.2 (0.5) kcal mol^{-1} $Å^{-1}$ for the calculations carried out in vacuum (water) [68,69]. Non-bonded cut-off distances were set at 8 Å. For calculations in water the Molecular Silverware algorithm (MS) [70] was used for solvation with periodic boundary conditions (PBC) in a canonical (NTV) ensemble.

The methods used for (i) the conformational study of the isolated N*m*βCD structures and (ii) the dimer $(N\textit{m}\beta CD)_2$ formation were similar to those described previously [31,32]. (i) For the isolated N*m*βCD, 5 ns MD simulations in the vacuum were made at several temperatures ranging from 350 to 600 K on each of the (10) initial N*m*βCD structures (Supporting Information, Fig. S11 and page 21). For these structures, in contrast with X*m*βCD which contain a xylylene moiety [31,32], the bulkier naphthyl moiety

characteristics and its substitution at the 1 and 8 naphthalene positions, only make two, *full-open* and *open*, conformations possible. Those capped conformations which appeared in X*m*βCD, for N*m*βCD are excluded [31,32]. (ii) Dimerization processes were performed starting from the minimized most stable *full-open* and *open* (Supporting Information, named 1 and 2, Fig. S11) N*m*βCD structures by considering three different CD-to-CD approaching, named *HH*, *HT* and *TT*-type (*H* = head; *T* = tail) (coordinate system to describe the approaching during dimerization process is depicted in Fig. S11). Critical analysis of the structures generated by scanning the θ [*O(4)–o–o′–O(4′)*] dihedral angle in the −180 to 180° range (10° intervals), the ε [*o–o′–O(4′)*] angle from 50 to 130° (10° intervals) and the *y* coordinate (*oo′* distance) from 20 to 6 Å (1 Å intervals) in the vacuum, followed by optimization (0.2 kcal mol^{-1} Å^{-1}) provided the most favourable θ and ε angles for approaching. Initially fixed these θ and ε angles at those values, the dimerization was emulated by approaching in 0.5 Å steps along the *y* coordinate from 20 to 6 Å now in the presence of water (MS, PBC, NVT). Every structure was optimized (1.0 kcal mol^{-1} Å^{-1}) and saved for further analysis. Minima binding energy (MBE) structures for dimers were optimized once again (0.5 kcal mol^{-1} Å^{-1}) and used as the starting conformations for the 1.0 ns MD simulations following the same strategy described earlier (Supporting Information, page 21) [31,32].

3.6.1. Conformational study of N*m*βCD

Probability distribution for ϕ_i and ψ_i torsional angles of the N*m*βCD macroring was obtained from the analysis of the 10 ns molecular dynamics trajectories in the vacuum at different temperatures on ten most stable structures for N*m*βCD (Fig. S11, Supporting Information). These structures were *full-open* or *open*. The ϕ_i and ψ_i angles for these structures like to adopt two typical skewing conformations from the *trans* state (0 ± 60°). However, ψ_i can visit a *cis* state (180°) for some of the glucopyranose units. This state is mostly responsible for the macroring distortion [31,32,67]. At any temperature and due to larger substituent size, the N*m*βCD macroring is much less flexible than its X*m*βCDs partner [31]. Therefore, the distributions for ϕ_i and ψ torsional angles only get slightly wider upon increasing the temperature. The angles that describe the rotation around the ether type bonds that link the naphthyl moiety to the macroring (an example of the probability distributions depicted in Fig. S12, Supporting Information) change from the initial placements during the MD trajectory. However, this does not make substantial changes in the N*m*βCD initial *full-open* or *open* conformations.

The distributions of the distances between the center of mass of the naphthyl moiety and βCD macroring show single maxima at any temperature (Fig. S13, Supporting Information). The average of these distances only slightly increases with temperature. These distributions do not show any isosbestic points due the presence of a *half-open*/*capped* equilibrium, as was previously observed for the X*m*βCD partner [31]. Here, the N*m*βCD system is more rigid and, as stated before, no significant changes from the initial existing conformations were observed. This probably contribute to the large stabilization for (N*m*βCD)$_2$.

Fig. 7 depicts the distribution of the angles between the 7-fold macro-ring CD axis and the ^1B_b and ^1L_a dipole transition moments obtained from the analysis of the MD trajectories in vacuum for the *open* (2) conformation (Fig. S11, Supporting Information) of N*m*βCD at two temperatures. Presumably, *open* conformations should be

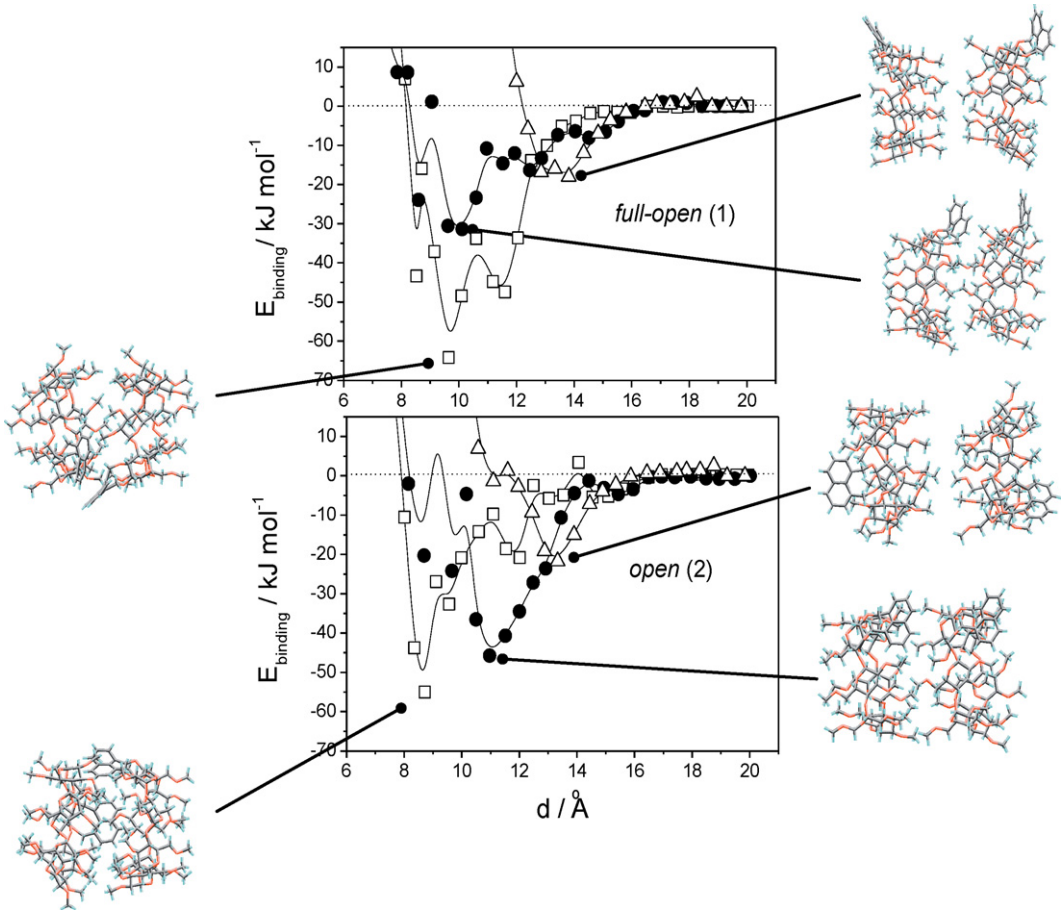

Fig. 8. Changes in the binding energies when a second N*m*βCD approaches a N*m*βCD (*y* coordinate in Å) by *HH* (□), *HT* (●) and *TT* (△) orientations for the most stable *full-open* (1) and *half-open* (2) conformations. Superimposed are the MBE (N*m*βCD)$_2$ structures.

responsible for the ICD signal since it is unlikely that the naphthyl group interacts with the CD cavity in the *full-open* arrangement. The distribution presents a maximum at $89 \pm 19^\circ$ ($26 \pm 23^\circ$) for ^1B_b (^1L_a) transition at 350 K. At 600 K, due to the larger conformational sampling, the distributions are wider and show a maximum located at $99 \pm 28^\circ$ or even become bimodal for the angle with ^1L_a (and ^1L_b), with the maxima placed at $27 \pm 24^\circ$ and $107 \pm 38^\circ$. The NMR experiments in deuterated chloroform, where only monomer exists, also point to a likely *open* conformation for N*m*βCD. The results of these distributions support the high intensity and positive sign of the ^1B_b ICD band for N*m*βCD in non-polar solvents when the only species present in the medium is the monomer and do not disagree with the sign and low intensity for the ^1L_b (and ^1L_a) band according to Kodaka's rules [57,58].

3.6.2. *Dimerization of NmβCD to (NmβCD)$_2$*

Fig. 8 depicts the changes in the interaction energy for the dimer formation as a function of the distance along the *y* coordinate (*d*, Å) between the centers of both N*m*βCDs for different *HH*, *HT* and *TT*-type approaches, for the most stable *full-open* (1) and *open* (2) conformations (Supporting Information, named 1 and 2, Fig. S11,). Although quantitatively different, whatever the orientation of the approaching is, both conformations shown favourable interactions at the MBE. Nevertheless, dimers formed by *HH* approaching are the most energetically favourable. This conformation accords with the EC dual signal observed in the ICD spectrum in water, which requires the two relatively close naphthyl groups to interact. It also is in agreement with the recent calculations done before for other similar naphthalene-modified CDs, where the chromophore is linked to a single glucopyranose position positioned in the secondary rim [71]. Van der Waals attractive interactions are the most important contribution for any of the *HH*, *HT* and *TT*-type dimers whatever the initial *full-open* (1) or *half-open* (2) conformations were. However, differently to X*m*βCD self-association [31], the electrostatic contributions are also significant especially when both CDs approach *HH* oriented. These results agree with the experimental $\Delta H < 0$ which is the typical sign for attractive van der Waals and/or electrostatics interactions.

Table 2 collects some geometrical parameters and different interaction energy contributions that involve the naphthyl moieties of both CDs at the MBE. These contributions are favourable in most of the cases, except for *TT* approaching, where these interactions obviously do not exist. It is noticeable that the inter-naphthyl distance nearly fulfills the EC requirements for both (1) and (2) *HH*-type dimer conformations at the *MBE*. Superimposed in Fig. 8 are the MBE structures for both orientations of the *HH*, *HT* and *TT* (N*m*βCD)$_2$ dimers that, once optimized again (0.5 kcal mol^{-1} Å^{-1}), were used as starting structures for MD simulations.

Fig. 9 shows the history of the binding energies between N*m*βCD units for (N*m*βCD)$_2$ dimers obtained from analysis of the 1.0 ns MD trajectories, as well as the distances between the center of mass of each N*m*βCD unit (Fig. S14 contains histories for other energetic interactions, Supporting Information). Table 2 also collects in parentheses the values of some of the parameters obtained for the minima binding energy structures achieved from the analysis of these trajectories. Again *HH* approaching is energetically more favourable than any other orientation. *HT*-dimers are stable during the whole 1 ns trajectory; *TT*-dimers, whatever the initial conformation was, dissociate reaching distances where CDs hardly interact. As collected in Table 2, the interaction energies for

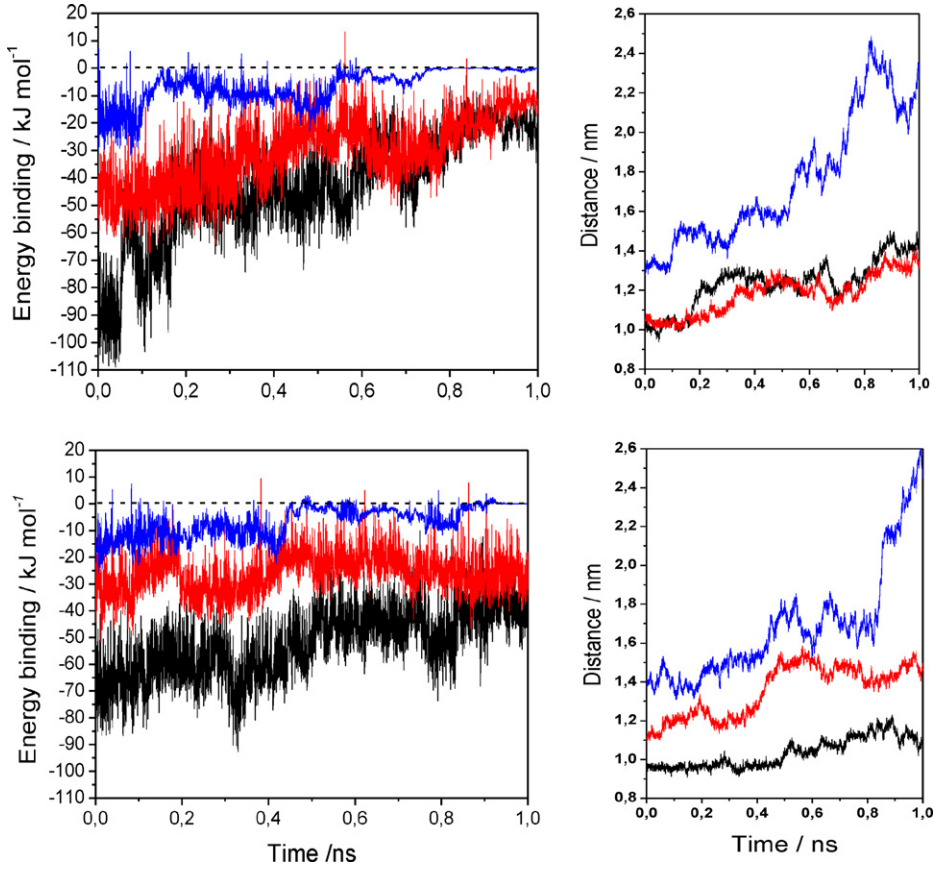

Fig. 9. Histories for CD–CD binding energies and center of mass distances for (N*m*βCD)$_2$ dimers by *HH* (black), *HT* (light gray) and *TT* (gray) orientations starting from the minimized MBE structures obtained from MM calculations for the most stable *full-open* (1) (upper panels) and *half-open* (2) (bottom panels) conformations.

Table 2
Binding energy and other contributions (kJ mol^{-1}), as well as, several geometrical parameters for the structures 1 and 2 of *MBE* for N*m*βCD by *HH*, *HT* and *TT* approaching obtained by MM calculations. In parentheses are the structures for minima binding energy obtained from the analysis of the 1 ns MD trajectories in the presence of water as a solvent.

Parameter	*HH*(1)	*HT*(1)	*TT*(1)	*HH*(2)	*HT*(2)	*TT*(2)
Distance CD–CD (Å)	9.6 (9.8)	10.1 (10.0)	13.8 (13.3)	8.7 (9.6)	11.0 (11.2)	13.3 (13.9)
Distance N1–N2 (Å)	4.9 (5.1)	8.5 (10.3)	21.8 (19.5)	6.8 (7.5)	10.6 (10.4)	22.5 (24.0)
θ (°)	11.2 (18.2)	0.1 (−133.4)	13.4 (26.4)	40.3 (25.6)	0.3 (−171.5)	19.3 (14.7)
$E_{binding}$ (kJ mol^{-1})	−64.2 (−108.9)	−31.4 (−67.2)	−17.8 (−31.8)	−55.0 (−93.7)	−45.8 (−51.6)	−21.7 (−25.8)
Electrostatics	−11.0 (−17.5)	−2.8 (−4.4)	+5.0 (+4.3)	−20.8 (−11.1)	−3.3 (+5.4)	2.0 (−1.3)
van der Waals	−53.1 (−91.4)	−28.5 (−62.8)	−22.9 (−36.1)	−34.3 (−82.7)	−42.5 (−57.0)	−27.0 (−24.5)
E_{inter} N2–N*m*CD1	−49.9 (−44.5)	−0.2 (−6.9)	0 (0)	−37.3 (−17.3)	−4.3 (−13.5)	0 (0)
E_{inter} N1–N*m*CD2	−41.8 (−61.0)	−12.1 (−5.3)	0 (0)	−18.5 (−23.4)	−23.6 (−2.2)	0 (0)
E_{inter} N1–N2	−29.4 (−36.4)	+0.6 (−1.0)	0 (0)	−8.4 (−12.3)	−3.5 (−3.8)	0 (0)

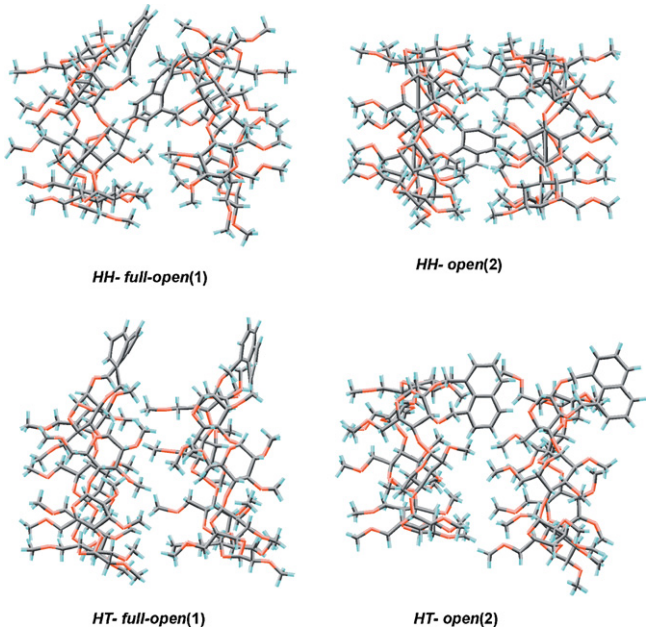

Fig. 10. Minima binding energy structures *HH-type* (upper) and *HT-type* (bottom) for (N*m*βCD)$_2$ dimer obtained from the analysis of the 1 ns MD simulations. Starting conformations were *full-open* (1) and *open* (2).

the MBE structures where naphthyl groups are involved, when they exist, were always more favourable when two N*m*βCD approach *HH* oriented.

Minima binding energy *HH* and *HT-type* structures for the (N*m*βCD)$_2$ dimer obtained from the analysis of the 1 ns MD simulations are depicted in Fig. 10. This *HH*-open(2) dimer structure would agree with most of the experimental findings. For this arrangement the centers of both naphthalene rings are separated by 7.5 Å and whereas the naphthalene rings are nearly parallels and favourably interact, they are far away from a face-to-face stacked structure.

4. Conclusion

NMR, fluorescence, induced circular dichroism and molecular modelling techniques were used for studying the self-aggregation of N*m*βCD in water and organic solvents. Dimerization constants in water are three orders of magnitude larger than those previously obtained for similar β-cyclodextrin derivatives bearing double-linked xylynene moiety at the secondary ring, instead of the naphthyl one. Dimerization processes were both enthalpy and entropy favoured. The $\Delta H < 0$ values are quite similar to those obtained for the (X*m*βCD)$_2$ formation. However, $\Delta S > 0$ in contrast with the negative value obtained for X*m*βCD (and also X*m*αCD and X*m*γCD [31,32]). This sign is attributed to the much higher loss of solvation order during dimerization in the case of the larger naphthyl groups compared with the benzene rings. NMR, ICD and fluorescence measurements indicate that dimerization takes place in high polar solvents. Similarly to that described for compounds in the xylylene-capped series [30–32] a negative solubility coefficient for N*m*βCD was observed in water. This fact is compatible with a change in hydration status that is strongly dependent on temperature. Considering the highly hydrophobic character of the naphthalene platform, it is conceivable that this moiety is shielded from bulk water at low temperatures in the dimer form and becomes exposed when increasing the molecular mobility in the monomer at the highest temperatures.

MD calculations of N*m*βCD allow us to infer that the conformations possible for the appended groups are those that are *open* or *full-open* and the absence of any *open* ⇌ *capped* equilibrium. Theoretical results, in agreement with NMR spectra, the exciton coupling bisignal obtained in the ICD spectrum and quenching experiments in water, indicated that most stable and probable dimers are formed when both N*m*βCD approach head-to-head with both CDs placed in an *open* conformation. Nevertheless, calculations do not exclude the presence of head-to-tail ones. For these (N*m*βCD)$_2$ structures the naphthyl moieties are relatively close to each other to couple their transition moments but without forming excimers and, although they do not penetrate inside the cavity of the neighbour CD, they may be relatively shielded from the solvent.

Acknowledgements

This work was supported by the Spanish MICINN (projects CTQ2008-03149/BQU and CTQ2010-15848/BQU), the EU (FEDER) and the Junta de Andalucía. M.J.G-A acknowledge FPU MICINN grants. FM and M.J.G-A acknowledge the assistance of M.L. Heijnen with the preparation of the manuscript.

Appendix A. Supplementary data

Supplementary data associated with this article can be found, in the online version, at doi:10.1016/j.jphotochem.2011.07.013.

References

[1] A. Douhal, Cyclodextrins Materials Photochemistry, Photophysics and Photobiology, Elsevier, Amsterdam, 2006.
[2] H. Dodziuk, Cyclodextrins and Their Complexes, Wiley-VCH Verlag GmbH & Co. KGaA, 2008.
[3] S. Li, W.C. Purdy, Cyclodextrins and their applications in analytical chemistry, Chem. Rev. 92 (1992) 1457–1470.
[4] E. Engeldinger, D. Armspach, D. Matt, Capped cyclodextrins, Chem. Rev. 103 (2003) 4147–4173.
[5] A.R. Khan, P. Forgo, K.J. Stine, V.T. D'Souza, Methods for selective modifications of cyclodextrins, Chem. Rev. 98 (1998) 1977–1996.
[6] H.H. Sigurdsson, E. Stefansson, E. Gudmundsdottir, T. Eysteinsson, M. Thorsteinsdottir, T. Loftsson, Cyclodextrin formulation of dorzolamide and its distribution in the eye after topical administration, J. Control. Release 102 (2005) 255–262.

[7] R.I. Gelb, L.M. Schwartz, Complexation of adamantane–ammonium substrates by β-cyclodextrin and its O-methylated derivatives, J. Inclusion Phenom. Mol. Recognit. Chem. 7 (1989) 537–543.
[8] J. Shi, D.-S. Guo, F. Ding, Y. Liu, Unique regioselective binding of permethylated β-cyclodextrin with azobenzene derivatives, Eur. J. Org. Chem. 92 (2009) 3–931.
[9] Y. Liu, J. Shi, D.-S. Guo, Novel permethylated β-cyclodextrin derivatives appended with chromophores as efficient fluorescent sensors for the molecular recognition of bile salts, J. Org. Chem. 72 (2007) 8227–8234.
[10] T. Ogoshi, A. Harada, Chemical sensors based on cyclodextrin derivatives, Sensors 8 (2008) 4961–4982.
[11] Y. Zhao, J. Gu, S.M. Chi, Y.C. Yang, H.Y. Zhu, Y.F. Wang, J.H. Liu, R. Huang, Aromatic diamino-bridged bis(β-cyclodextrin) as fluorescent sensor for the molecular recognition of bile salts, Bull. Korean Chem. Soc. 29 (2008) 2119–2124.
[12] X.-L. Chen, L.-B. Qu, T. Zhang, H. Liu, F. Yu, Y.-Z. Yu, Y.-F. Zhao, Direct observation of non-covalent complexes formed through phosphorylated flavonoid protein interaction by electrospray ionization mass spectrometry, Supramol. Chem. 16 (2004) 67–75.
[13] A. Ueno, T. Kuwabara, A. Nakamura, F. Toda, A modified cyclodextrin as a guest responsive color-change indicator, Nature 356 (1992) 136–137.
[14] P.F. Wang, L. Jullien, B. Valeur, J.S. Filhol, J. Canceill, J.M. Lehn, Multichromophoric cyclodextrins. 5. Antenna-induced unimolecular photoreactions. Photoisomerization of a nitrone, New J. Chem. 20 (1996) 895–907.
[15] J.W. Park, H.E. Song, S.Y. Lee, Homo-dimerization and hetero-association of 6-O-(2-sulfonato-6-naphthyl)-β-cyclodextrin and 6-deoxy-(pyrene-1-carboxamido)-β-cyclodextrin, J. Org. Chem. 68 (2003) 7071–7076.
[16] S.R. McAlpine, M.A. Garcia-Garibay, Studies of naphthyl-substituted β-cyclodextrins. Self-aggregation and inclusion of external guests, J. Am. Chem. Soc. 120 (1998) 4269–4275.
[17] X.-M. Gao, L.-H. Tong, Y.-L. Zhang, A.-Y. Hao, Y. Inoue, Exciton coupling and binding behavior of β-cyclodextrin substituted by one 2-naphthoyl moiety, Tetrahedron Lett. 40 (1999) 969–972.
[18] X.-M. Gao, Y.-L. Zhang, L.-H. Tong, Y.-H. Ye, X.-Y. Ma, W.-S. Liu, Y. Inoue, Exciton coupling and complexation behavior of β-cyclodextrin naphthoate, J. Incl. Phenom. Macrocycl. Chem. 39 (2001) 77–80.
[19] K.K. Park, Y.S. Kim, S.Y. Lee, H.E. Song, J.W. Park, Preparation and self-inclusion properties of p-xylylenediamine-modified β-cyclodextrins: dependence on the side of modification, J. Chem. Soc., Perkin Trans. 2 (2001) 2114–2118.
[20] J.W. Park, S.Y. Lee, S.M. Kim, Efficient inclusion complexation and intracomplex excitation energy transfer between aromatic group-modified β-cyclodextrins and a hemicyanine dye, J. Photochem. Photobiol. A 173 (2005) 271–278.
[21] F. Moriwaki, H. Kaneko, A. Ueno, T. Osa, F. Hamada, K. Murai, Excimer formation and induced-fit type of complexation of β-cyclodextrin capped by two naphthyl moieties, Bull. Chem. Soc. Jpn. 60 (1987) 3619–3623.
[22] A. Ueno, F. Moriwaki, T. Osa, F. Hamada, K. Murai, Fluorescence and circular dichroism studies on host-guest complexation of β-cyclodextrin bearing two 2-naphthyl moieties, Bull. Chem. Soc. Jpn. 59 (1986) 465–470.
[23] M.N. Berberan-Santos, J. Canceill, J.C. Brochon, L. Jullien, J.M. Lehn, J. Pouget, P. Tauc, B. Valeur, Multichromophoric cyclodextrins. 1. Synthesis of O-naphthoyl-β-cyclodextrins and investigation of excimer formation and energy hopping, J. Am. Chem. Soc. 114 (1992) 6427–6436.
[24] M.N. Berberan-Santos, J. Pouget, B. Valeur, J. Canceill, L. Jullien, J.M. Lehn, Multichromophoric cyclodextrins. 2. Inhomogeneous spectral broadening and directed energy hopping, J. Phys. Chem. 97 (1993) 11376–11379.
[25] M.N. Berberan-Santos, J. Canceill, E. Gratton, L. Jullien, J.-M. Lehn, P. So, J. Sutin, B. Valeur, Multichromophoric cyclodextrins. 3. Investigation of dynamics of energy hopping by frequency-domain fluorometry, J. Phys. Chem. 100 (1996) 15–20.
[26] S.R. McAlpine, M.A. Garcia-Garibay, Binding studies of adamantanecarboxylic acid and a naphthyl-bound β-cyclodextrin by variable temperature ^{1}H NMR, J. Org. Chem. 61 (1996) 8307–8309.
[27] S.R. McAlpine, M.A. Garcia-Garibay, Inside–outside isomerism of β-cyclodextrin covalently linked with a naphthyl group, J. Am. Chem. Soc. 118 (1996) 2750–2751.
[28] J.W. Park, H.E. Song, S.Y. Lee, Face selectivity of inclusion complexation of viologens with β-cyclodextrin and 6-O-(2-sulfonato-6-naphthyl)-γ-cyclodextrin, J. Phys. Chem. B 106 (2002) 7186–7192.
[29] J.W. Park, H.E. Song, S.Y. Lee, Facile dimerization and circular dichroism characteristics of 6-O-(2-sulfonato-6-naphthyl)-β-cyclodextrin, J. Phys. Chem. B 106 (2002) 5177–5183.
[30] P. Balbuena, D. Lesur, M.J. González-Álvarez, F. Mendicuti, C. Ortiz Mellet, J.M. García Fernández, One-pot regioselective synthesis of 2I,3I-O-(o-xylylene)-capped cyclomalto-oligosaccharides: tailoring the topology and supramolecular properties of cyclodextrins, Chem. Commun. 327 (2007) 0–3272.
[31] M.J. González-Álvarez, P. Balbuena, C. Ortiz Mellet, J.M. García Fernández, F. Mendicuti, Study of the conformational and self-aggregation properties of 2I,3I-O-(o-xylylene)-per-O-Me-α- and -β-cyclodextrins by fluorescence and molecular modelling, J. Phys. Chem. B 112 (2008) 13717–13729.
[32] M.J. González-Álvarez, J. Vicente, C. Ortiz Mellet, J.M. García Fernández, F. Mendicuti, Thermodynamics of the dimer formation of 2I,3I-O-(o-xylylene)-per-O-Me-β-cyclodextrin: fluorescence, molecular mechanics and molecular dynamics, J. Fluoresc. 19 (2009) 975–988.
[33] K. Uekama, T. Irie, in: D. Duchême (Ed.), Cyclodextrins and Their Industrial Uses, Edition Sante, Paris, 1987, pp. 393–439.
[34] K. Harata, X-ray structures of hexakis(2,6-di-O-methyl)-β-cyclodextrin in two crystal forms, Supramol. Chem. 5 (1995) 231–236.
[35] T. Steiner, F. Hirayama, W. Saenger, Topography of cyclodextrin inclusion complexes. Part 40. Crystal structures of hexakis-(2,6-di-O-methyl)-cyclomaltohexaose (dimethyl-β-cyclodextrin) crystallized from acetone, and crystallized from hot water, Carbohydr. Res. 296 (1996) 69–82.
[36] T. Steiner, W. Saenger, Topography of cyclodextrin inclusion complexes. Part 37. Crystal structure of anhydrous heptakis-(2,6-di-O-methyl) cyclomaltoheptaose (dimethy-β-cyclodextrin), Carbohydr. Res. 275 (1995) 73–82.
[37] T. Steiner, W. Saenger, Crystal structure of anhydrous hexakis(2,3,6-tri-O-methyl)cyclomaltohexaose (permethyl-β-cyclodextrin) grown from hot water and from cold NaCl solutions, Carbohydr. Res. 282 (1996) 53–63.
[38] T. Aree, I. Uson, B. Schulz, G. Reck, H. Hoier, G.M. Sheldrick, W. Saenger, Variation of a theme crystal structure with four octakis(2,3,6-tri-O-methyl)-β-cyclodextrin molecules hydrated differently by a total of 19.3 water, J. Am. Chem. Soc. 121 (1999) 3321–3327.
[39] T. Steiner, W. Saenger, Topography of cyclodextrin inclusion complexes. Part 43. Closure of the cavity in permethylated cyclodextrins through glucose inversion, flipping, and kinking, Angew. Chem., Int. Ed. 37 (1999) 3404–3407.
[40] T. Aree, H. Hoier, B. Schulz, G. Reck, W. Saenger, Novel type of thermostable channel clathrate hydrate formed by heptakis(2,6-di-O-methyl)-β-cyclodextrin·15H_2O—a paradigm of the hydrophobic effect, Angew. Chem., Int. Ed. 39 (2000) 897–899.
[41] M.R. Caira, V.J. Griffith, L.R. Nassimbeni, O.B. van, Unusual 1C4 conformation of a methylglucose residue in crystalline permethyl-β-cyclodextrin monohydrate, J. Chem. Soc., Perkin Trans. 2 (1994) 2071–2072.
[42] The authors kindly thank Dr. C. Hunter for providing the titration isotherm curve fitting program. For detailed description of the fitting methods and equations, see:
(a) A.P. Bisson, C.A. Hunter, J.C. Morales, K. Young, Chem. Eur. J. 4 (1998) 845;
(b) A.P. Bisson, F.J. Carver, D.S. Eggleston, R.C. Haltiwanger, C.A. Hunter, D.L. Livingston, J.F. McCabe, C. Rotger, A.E. Rowan, J. Am. Chem. Soc. 122 (2000) 8856.
[43] N. Harting, G. Thielking, H.-F. Grutzmacher, Methoxymethyl group migration in bis(methoxymethyl)arene radical cations: a new outlook on the rearrangement of dialkylarene radical cations, Int. J. Mass Spectrom. Ion Processes 167/168 (33) (1997) 5–352.
[44] M.J. González-Álvarez, A. Di Marino, F. Mendicuti, Fluorescence induced circular dichroism and molecular mechanics of 1-methyl naphthalenecarboxylate complexes with 2-hydroxypropyl cyclodextrins, J. Fluoresc. 19 (2009) 449–462.
[45] K. Harata, H. Uedaira, Circular dichroism spectra of the β-cyclodextrin complex with naphthalene derivatives, Bull. Chem. Soc. Jpn. 48 (1975) 375–378.
[46] J.R. Platt, Classification of spectra of cata-condensed hydrocarbons, J. Chem. Phys. 17 (1949) 484–495.
[47] D.V. O'Connor, W.R. Ware, J.C. Andre, Deconvolution of fluorescence decay curves. A critical comparison of techniques, J. Phys. Chem. 83 (1979) 1333–1343.
[48] F. Mendicuti, Applications of fluorescence techniques and modeling to the study of the complexation of chromophore-containing guests with cyclodextrins, Trends Phys. Chem. 11 (2006) 61–77.
[49] A. Di Marino, L. Rubio, F. Mendicuti, Fluorescence and molecular mechanics of 1-methyl naphthalenecarboxylate/cyclodextrin complexes in aqueous medium, J. Incl. Phenom. Macrocycl. Chem. 58 (2007) 103–114.
[50] A. Di Marino, F. Mendicuti, Fluorescence of the complexes of 2-methylnaphthoate and 2-hydroxypropyl-α, -β, and -γ-cyclodextrins in aqueous solution, Appl. Spectrosc. 56 (2002) 1579–1587.
[51] J.M. Madrid, F. Mendicuti, Thermodynamic parameters of the inclusion complexes of 2-methylnaphthoate and α- and β-cyclodextrins, Appl. Spectrosc. 51 (1997) 1621–1627.
[52] R.U. Lemieux, How water provides the impetus for molecular recognition in aqueous solution, Acc. Chem. Res. 29 (1996) 373–380.
[53] J.R. Lakowicz, Quenching of fluorescence, in: J.R. Lakowicz (Ed.), Principles of Fluorescence Spectroscopy, Springer, New York, 2008, p. 280.
[54] Y. Song, Y. Chen, Y. Liu, Switchable fluorescence behaviors of pyronine Y at different pH values upon complexation with biquinolino-bridged bis(β-cyclodextrin), Photochem. Photobiol. A 173 (2005) 328–333.
[55] T. Aoyagi, A. Nakamura, H. Ikeda, T. Ikeda, H. Mihara, A. Ueno, Alizarin yellow-modified β-cyclodextrin as a guest-responsive absorption change sensor, Anal. Chem. 69 (1997) 659–663.
[56] T. Kuwabara, H. Nakajima, M. Nanasawa, A. Ueno, Color change indicators for molecules using methyl red-modified cyclodextrins, Anal. Chem. 71 (1999) 2844–2849.
[57] M. Kodaka, Application of a general rule to induced circular dichroism of naphthalene derivatives complexed with cyclodextrins, J. Phys. Chem. A 102 (1998) 8101–8103.
[58] M. Kodaka, Sign of circular dichroism induced by β-cyclodextrin, J. Phys. Chem. 95 (1991) 2110–2112.
[59] M. Kodaka, A general rule for circular dichroism induced by a chiral macrocycle, J. Am. Chem. Soc. 115 (1993) 3702–3705.
[60] M. Kodaka, T. Fukaya, Complex formation between heptylviologen and cyclodextrin, Bull. Chem. Soc. Jpn. 59 (1986) 2032–2034.
[61] M. Kodaka, T. Fukaya, Induced circular dichroism spectrum of a β-cyclodextrin complex with heptylviologen, Bull. Chem. Soc. Jpn. 62 (1989) 1154–1157.
[62] N. Berova, K. Nakanishi, Exciton chirality method: principles and applications, in: N. Berova, K. Nakanishi, R.W. Woody (Eds.), Circular Dichroism: Principles and Applications, Wiley-VCH, 2000, pp. 337–382.

[63] A. Douhal, Breaking, making, and twisting of chemical bonds in gas, liquid, and nanocavities, Acc. Chem. Res. 37 (2004) 349–355.
[64] SYBYL St. Louis, Missouri, USA, 2007.
[65] M. Clark, R.D. Cramer III, O.N. Van, Validation of the general purpose Tripos 5.2 force field, J. Comput. Chem. 10 (1989) 982–1012.
[66] M.J. Frisch, et al., MOPAC (AM1) included in the Gaussian 03 Package, Gaussian, Inc., Wallingford, CT, 2004.
[67] J. Pozuelo, J.M. Madrid, F. Mendicuti, W.L. Mattice, Inclusion complexes of chain molecules with cycloamyloses. 1. Conformational analysis of the isolated cycloamyloses using molecular dynamics simulations, Comput. Theor. Polym. Sci. 6 (1996) 125–134.
[68] Y. Brunel, H. Faucher, D. Gagnaire, A. Rassat, Program of minimization of the empirical energy of a molecule by a simple method, Tetrahedron 31 (1975) 1075–1091.
[69] W.H. Press, B.P. Flannery, S.A. Teukolski, W.T.E. Vetterling, Numerical Recipes: The Art of Scientific Computing, Cambridge University Press, 1988.
[70] M. Blanco, Molecular silverware. I. General solutions to excluded volume constrained problems, J. Comput. Chem. 12 (1991) 237–247 (2 plates).
[71] M.R. Gamieldien, I. Maestre, C. Jaime, K.J. Naidoo, Optimal configurations of capped β-cyclodextrin dimers in water maximise hydrophobic association, ChemPhysChem 11 (2010) 452–459.